Cell Research (2012) 22:1270-1284.

www.nature.com/cr

ORIGINAL ARTICLE

Nudel is crucial for the WAVE complex assembly *in vivo* by selectively promoting subcomplex stability and formation through direct interactions

Shuang Wu[1], Li Ma[1], Yibo Wu[2], Rong Zeng[2], Xueliang Zhu[1]

[1]State Key Laboratory of Cell Biology, Institute of Biochemistry and Cell Biology, Shanghai Institutes for Biological Sciences, Chinese Academy of Sciences, 320 Yue Yang Road, Shanghai 200031, China; [2]State Key Laboratory of Molecular Biology, Institute of Biochemistry and Cell Biology, Shanghai Institutes for Biological Sciences, Chinese Academy of Sciences, 320 Yue Yang Road, Shanghai 200031, China

The WAVE regulatory complex (WRC), consisting of WAVE, Sra, Nap, Abi, and HSPC300, activates the Arp2/3 complex to control branched actin polymerization in response to Rac activation. How the WRC is assembled *in vivo* is not clear. Here we show that Nudel, a protein critical for lamellipodia formation, dramatically stabilized the Sra1-Nap1-Abi1 complex against degradation in cells through a dynamic binding to Sra1, whereas its physical interaction with HSPC300 protected free HSPC300 from the proteasome-mediated degradation and stimulated the HSPC300-WAVE2 complex formation. By contrast, Nudel showed little or no interactions with the Sra1-Nap1-Abi1-WAVE2 and the Sra1-Nap1-Abi1-HSPC300 complexes as well as the mature WRC. Depletion of Nudel by RNAi led to general subunit degradation and markedly attenuated the levels of mature WRC. It also abolished the WRC-dependent actin polymerization *in vitro* and the Rac1-induced lamellipodial actin network formation during cell spreading. Therefore, Nudel is important for the early steps of the WRC assembly *in vivo* by antagonizing the instability of certain WRC subunits and subcomplexes.

***Keywords*:** Nudel; Sra1; HSPC300; the WAVE regulatory complex; assembly; stabilization

Cell Research (2012) **22**:1270-1284. doi:10.1038/cr.2012.47; published online 27 March 2012

Introduction

The WAVE regulatory complex (WRC) is a pentameric protein complex consisting of WAVE, Sra, Nap, Abi, and HSPC300 (also known as Brick1). It is an upstream activator of the Arp2/3 complex, an actin nucleation factor that facilitates the assembly of a dense meshwork of branched F-actin to sustain the leading edge projections, or lamellipodia, of migrating cells [1-3]. Paralogues for the WRC subunits are found in mammals. Of them, WAVE2, Sra1/PIR121, Nap1, Abi1-2 are ubiquitously expressed, whereas WAVE1 and 3, Abi3, and HEM1, the Nap1 homologue, are restricted to brain and/or hematopoietic tissue [3]. Nonetheless, although the complex repertoire may vary, all WRCs are believed to regulate actin nucleation activity of the Arp2/3 complex [2, 3].

The WRC is intrinsically inactive. WAVE (also known as Scar) belongs to the Wiskott-Aldrich syndrome protein (WASP) family, whose members bear a C-terminal VCA domain sufficient for activation of the Arp2/3 complex [4]. Unlike the autoinhibitory WASP and N-WASP, WAVE protein alone is active [5, 6]. A role of the WRC is thus to quench the constitutive activity of WAVE [4, 5, 7]. Recently, crystallography reveals that, in the WAVE1-containing WRC, the VCA region is indeed buried into the Sra1-Nap1 heterodimer [8]. Activation of the WRC, e.g., by its recruitment to the plasma membrane through interactions of the Sra1-Nap1 heterodimer with Rac-GTP and phospholipids, is thus believed to release the masked VCA domain [3-5, 8].

How the WRC is assembled *in vivo* is still poorly

Correspondence: Xueliang Zhu
Tel: +86 21 54921406; Fax: +86 21 54921011
E-mail: xlzhu@sibs.ac.cn
Received 23 September 2011; revised 6 February 2012; accepted 14 February 2012; published online 27 March 2012

understood. To prevent free subunits from malfunctioning, they may need to be either quickly assembled into the WRC or degraded. Indeed, free subunits are unstable and thus not detected in bulk except for HSPC300, which exists as homotrimers [3, 6, 9, 10]. Moreover, depletion of one subunit can concomitantly lead to proteasome-dependent degradation of the others, resulting in phenotypes similar to the repression of WAVE, e.g., lack of Rac-dependent lamellipodia formation [3, 6, 9, 11-13]. As nascent WRC is assembled from neosynthesized proteins [9], it is more likely to be formed from stable intermediate subcomplexes than from abrupt simultaneous assembly of unstable free subunits. A variety of subcomplexes from heterodimers to tetramers have been identified *in vitro* [4, 6, 8, 10]. In particular, functional WRC can be obtained by mixing Sra-Nap and WAVE-HSPC300-Abi complexes [4, 8]. Whether these subcomplexes exist *in vivo* and how they impact the WRC assembly, however, are not known.

Nudel (also named Ndel1) is a multifunctional protein critical for the cell migration and the cytoplasmic dynein-related cellular activities. Nudel RNAi seriously impairs lamellipodia formation [14, 15]. Mechanistic studies suggest two distinct but correlated functions at the leading edge of migrating cells. First, Nudel stabilizes Cdc42-GTP by sequestering the negative regulator Cdc42GAP and thus contributes to polarity formation [15, 16]. Second, it selectively strengthens nascent adhesions through interaction with Paxillin [14]. It is also required for nuclear translocation in migrating neurons during the development of central nervous system by positively regulating cytoplasmic dynein functions [17, 18]. Nudel is also a dynein-interacting protein important for a variety of dynein functions *in vivo*, including the vesicle transport, mitosis, and cell migration [15, 19-24]. In this report, we showed that Nudel is a key factor for the WRC assembly *in vivo* by facilitating formations of distinct stable subcomplexes and is thus critical for lamellipodial actin polymerization.

Results

Nudel directly interacts with Sra1 and HSPC300

Although our previous findings might explain why Nudel is critical for lamellipodia formation [14, 15], a more direct role of Nudel could not be excluded. To clarify this, we analyzed Nudel-associated proteins immunoprecipitated from mouse brain lysate [15] using the shotgun mass spectrometry. Among the 284 protein hits, including the known associated proteins, such as subunits of cytoplasmic dynein, Lis1, and 14-3-3 [15], three of the five subunits of the WRC (Figure 1A), Sra1, Nap1, and Abi1, were identified (Supplementary information, Table S1). Although HSPC300 has only ~75 residues and might be missed in the mass spectrometry, none of the WAVE1-3 [3] was detected. When HEK293T cell lysate ectopically expressing Flag-tagged Nudel was subjected to co-immunoprecipitation (co-IP) using the anti-Flag M2 resin, we readily detected Sra1, Nap1, Abi1, and HSPC300 by immunoblotting. WAVE2, however, was still undetectable (Figure 1B). Therefore, Nudel appears to associate with components of the WRC, but not the entire complex.

To further investigate the interplay between Nudel and the WRC, we ectopically coexpressed Flag-Nudel with HA-tagged WRC subunit in HEK293T cells and performed co-IP using the anti-Flag M2 resin. Immunoblotting showed that only HA-Sra1 and HA-HSPC300 associated with Nudel (Figure 1C, lanes 8 and 12). We then performed GST pull-down assays using GST-Nudel and polyhistidine (His)-tagged WRC subunits expressed in *E. coli* and confirmed the direct interaction of Nudel with Sra1 and HSPC300 (Supplementary information, Figure S1).

To further corroborate the above results, we performed co-IP using proteins purified from HEK293T cells and examined whether the immunoprecipitated proteins could be detected by the Coomassie Blue staining. As the bacterially expressed proteins often showed prominent degradations (Supplementary information, Figure S1), we purified HA-Sra1, Flag-Nudel, and Flag-luciferase from HEK293T cells after the ectopic expression. When HA-Sra1 was mixed with Flag-tagged Nudel or luciferase and subjected to co-IP using the anti-Flag M2 resin, Sra1 was only detected to associate with Nudel by both the Coomassie Blue staining and immunoblotting (Figure 1D). We then similarly purified HA-luciferase and HA-HSPC300 from HEK293T cells and mixed them with purified Flag-Nudel, respectively. Co-IP using the anti-HA resin followed by the Coomassie Blue staining and immunoblotting indicated that Nudel only interacted with HSPC300, but not luciferase (Figure 1E). Domain-mapping experiments using different Nudel mutants suggested specific interactions of Sra1 and HSPC300 with the C-terminal regions of Nudel (Supplementary information, Figure S2). Nevertheless, HSPC300 bound to the Nudel^{P2C} mutant, whereas Sra1 did not (Supplementary information, Figure S2A, S2B, lane 5 and S2C, lane 7). Thus, the interaction domains of Nudel for the two proteins might overlap but are not identical.

Taken together, these results indicate a strong physical interaction of Nudel with Sra1 and HSPC300. The Nap1 and Abi1 detected in the co-IP (Figure 1B; Supplementary information, Table S1) may thus associate with Nudel

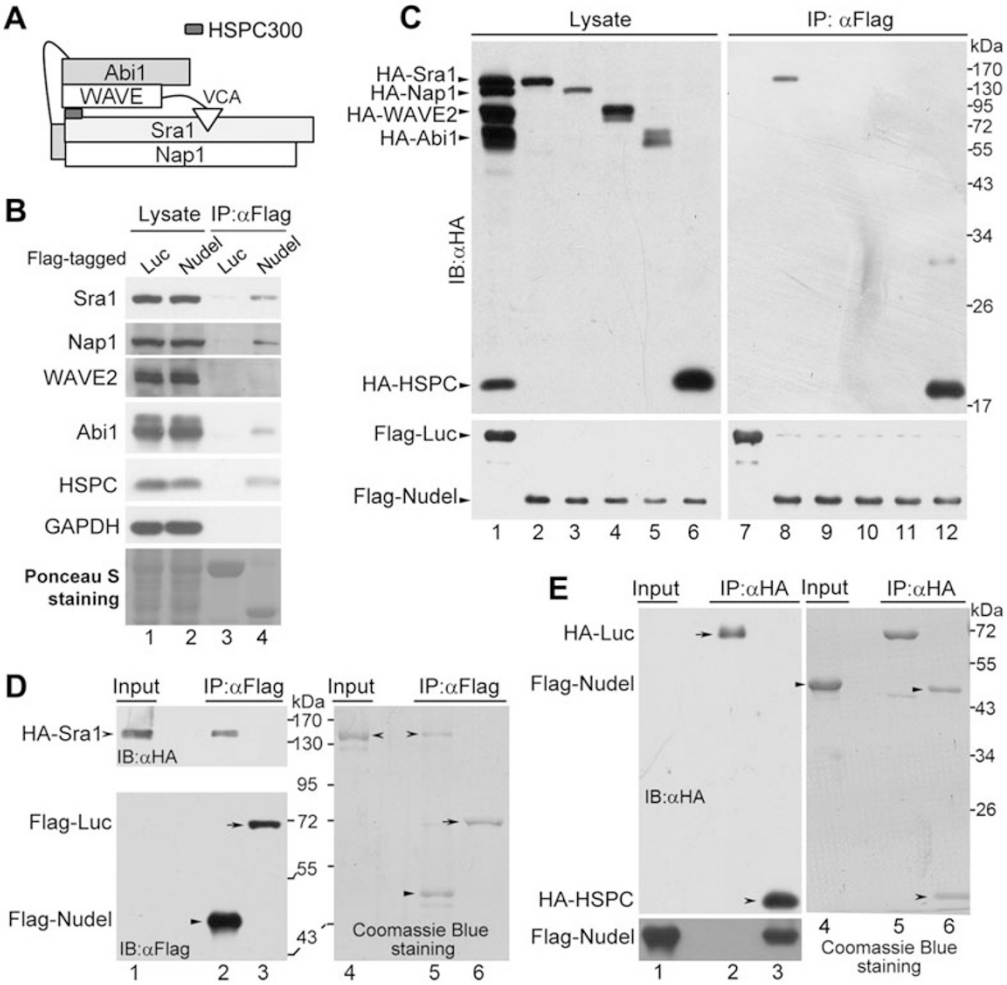

Figure 1 Interactions between Nudel and the WRC subunits. **(A)** A schematic architecture of the WRC, mainly based on crystal structure [8]. **(B)** The associations of the WRC subunits with Nudel *in vivo*. HEK293T cells ectopically expressing Flag-tagged Nudel or firefly luciferase were lysed and subjected to co-IP using the anti-Flag M2 resin. Immunoblotting (IB) was then performed to visualize the indicated proteins, except that the Ponceau S staining of a blot showed the Flag-tagged proteins (lanes 3 and 4). **(C)** The association between individual WRC subunits and Flag-Nudel. The indicated HA-tagged WRC subunits were coexpressed ectopically with Flag-tagged Nudel or luciferase in HEK293T cells (lanes 1-6). Co-IP was then performed using the anti-Flag M2 resin (lanes 7-12). **(D)** The direct interaction between Nudel and Sra1. HA-Sra1 ectopically expressed in HEK293T cells was absorbed on the anti-HA resin and then eluted with the HA peptide. The WRC in the eluted proteins was further depleted via incubation with anti-Abi1 antibody immobilized on protein G beads for 1 h. The same amount of the purified HA-Sra1 (lanes 1 and 4) was mixed with Flag-Nudel or Flag-luciferase that was expressed in HEK293T cells and immobilized on the anti-Flag M2 resin. After further incubation on ice for 2 h, the bound proteins were eluted with the Flag peptide. The eluted proteins were visualized by immunoblotting (lanes 2 and 3) and Coomassie Blue staining (lanes 5 and 6) after the SDS-PAGE. **(E)** The direct interaction between Nudel and HSPC300. Flag-Nudel ectopically expressed in HEK293T cells was purified using the anti-Flag M2 resin and eluted with the Flag peptide (lanes 1 and 4). HA-luciferase and HA-HSPC300 expressed in HEK293T cells were immobilized on the anti-HA resin, respectively, and mixed with the same amount of the purified Flag-Nudel. After further incubation on ice for 2 h, the bound proteins were eluted with the HA peptide. The eluted proteins were visualized by immunoblotting (lanes 2 and 3) and Coomassie Blue staining (lanes 5 and 6) after the SDS-PAGE.

indirectly through subcomplex(es).

Nudel preferably associates with the S-N-A complex in a WAVE2-sensitive manner

To understand what subcomplex(es) of the WRC interact with Nudel, we first examined interplays

between Nudel and the Sra1-related subcomplexes. As the endogenous WRC subunits are believed to exist mostly in the form of the mature WRC [3, 6, 9, 10], we transiently overexpressed different subunits to facilitate the formation and thus the detection of possible nascent subcomplexes in cells. We also managed to express HA-tagged Sra1, Nap1, Abi1, and WAVE2 to similar levels, either individually or in different combinations, together with Flag-Nudel, in HEK293T cells (Figure 2A). The expression levels of exogenous proteins relative to endogenous ones were estimated to be between ~0.7-4.5-fold for Sra1, Nap1, and Abi1 (Supplementary information, Figure S3A and S3B). The level of endogenous WAVE2, however, was much lower than that of HA-WAVE2 (Supplementary information, Figure S3A and S3B), suggesting that its steady-state level is much lower than those of the other three in HEK293T cells. Co-IP using the anti-Flag resin revealed that when these subunits were overexpressed individually or each with Sra1, only Sra1 was detected in association with Nudel (Figure 2A, lanes 2-8; Supplementary information, Figure S3A, lanes 14-20). We then coexpressed two subunits with Sra1, and found that the combination of Sra1, Nap1, and Abi1 induced a robust synergistic effect on their associations with Nudel (Figure 2A, lanes 9-11; Supplementary information, Figure S3A). The interaction was so strong that, prior to immunostaining, the Sra1 and Nap1 bands on the blots were easily visualized by the Ponceau S staining (Supplementary information, Figure S3A, lane 22). Further overexpression of WAVE2 repressed such associations (Figure 2A, lane 12; Supplementary information, Figure S3A, lane 24).

Nudel has little effect on the assembly of the S-N-A complex

We then investigated why Nudel preferably interacts with the S-N-A complex. To test whether Nudel could facilitate such complex formation, HA-tagged Sra1, Nap1, WAVE2, and Nudel were overexpressed to similar levels in HEK293T cells as shown in Figure 2B (lanes 1-5), together with Flag-Abi1. Co-IP using the anti-Flag resin confirmed the existence of the S-N-A complex, since Sra1 and Nap1 showed similar stoichiometry in the immunocomplex (Figure 2B, lane 7). As reported [6, 10], the S-N-A-W complex formed when HA-WAVE2 was further expressed (Figure 2B, lane 8). Further overexpression of HA-Nudel (Figure 2B, lanes 4, 5), however, did not significantly affect the levels of the above complexes (lanes 9, 10 vs 7, 8), indicating that Nudel does not facilitate the S-N-A complex formation. Interestingly, Nudel did not show a very tight association with the S-N-A complex because it was only detected with anti-HA monoclonal antibody after long exposure (Figure 2B, lane 9). Its association with the S-N-A-W complex, however, was even weaker (Figure 2B, lane 10 vs 9).

Nudel stabilizes the S-N-A complex against degradation

In the above experiments we noticed that in order to obtain similar levels of exogenous Sra1 and Nap1, higher amount of expression plasmids was often needed in the absence of exogenous Nudel (Figure 2B, lanes 2, 3 vs 4, 5). We thus tested whether Nudel is able to prevent the S-N-A complex from degradation. Cells were then transfected with fixed amount of each expression plasmid, and GFP was used as an internal control of the transfection efficiency for all the samples (Figure 2C). Immunoblotting indicated that the overexpression of Nudel with Sra1, Nap1, and Abi1 indeed significantly elevated levels of the latter three proteins (Figure 2C, lanes 6 vs 5; Figure 2D). In contrast, the effect of Nudel was not prominent on Abi1 alone (Figure 2C, lanes 2 vs 1) or even Abi1 and Nap1 (lanes 4 vs 3).

To confirm that Nudel has a role in stabilizing the S-N-A subcomplex, we assessed its effect on the half-life of the complex. We transfected HEK293T cells as indicated in Figure 2C, except that Flag-luciferase was ectopically expressed in control cells. When cells were treated with cycloheximide (Chx) to block protein synthesis [25], HA-tagged Sra1, Nap1, and Abi1 showed increased stability in the presence of Flag-Nudel (Figure 2E). When the relative levels of HA-Abi1 were quantified, its half-life was estimated to increase from an average of 8.4 min to 30.7 min (Figure 2F).

Nudel protects HSPC300 from the proteasome-mediated degradation

As HSPC300 was also co-immunoprecipitated with Nudel (Figure 1B), we examined whether Nudel could stabilize HSPC300 as well. Indeed, its overexpression tremendously increased the levels of the exogenous HSPC300 (Figure 3A, lanes 1, 2 and 5, 6). Inhibition of the proteasome activity by the MG132 treatment for 12 h fully rescued the HSPC300 levels at 24 h post transfection (Figure 3A, lanes 3, 4), suggesting a rapid degradation of HSPC300 by the proteasome in the absence of Nudel. The rescue was partial at 48 h (Figure 3A, lanes 7, 8), possibly due to the remarkable differences in protein levels prior to the addition of MG132 (lanes 5, 6). Moreover, when the Nudel mutants incapable of binding to HSPC300 (Supplementary information, Figure S2) were ectopically coexpressed with HA-HSPC300, they all failed to stabilize HA-HSPC300 (Figure 3B), indicating the importance of

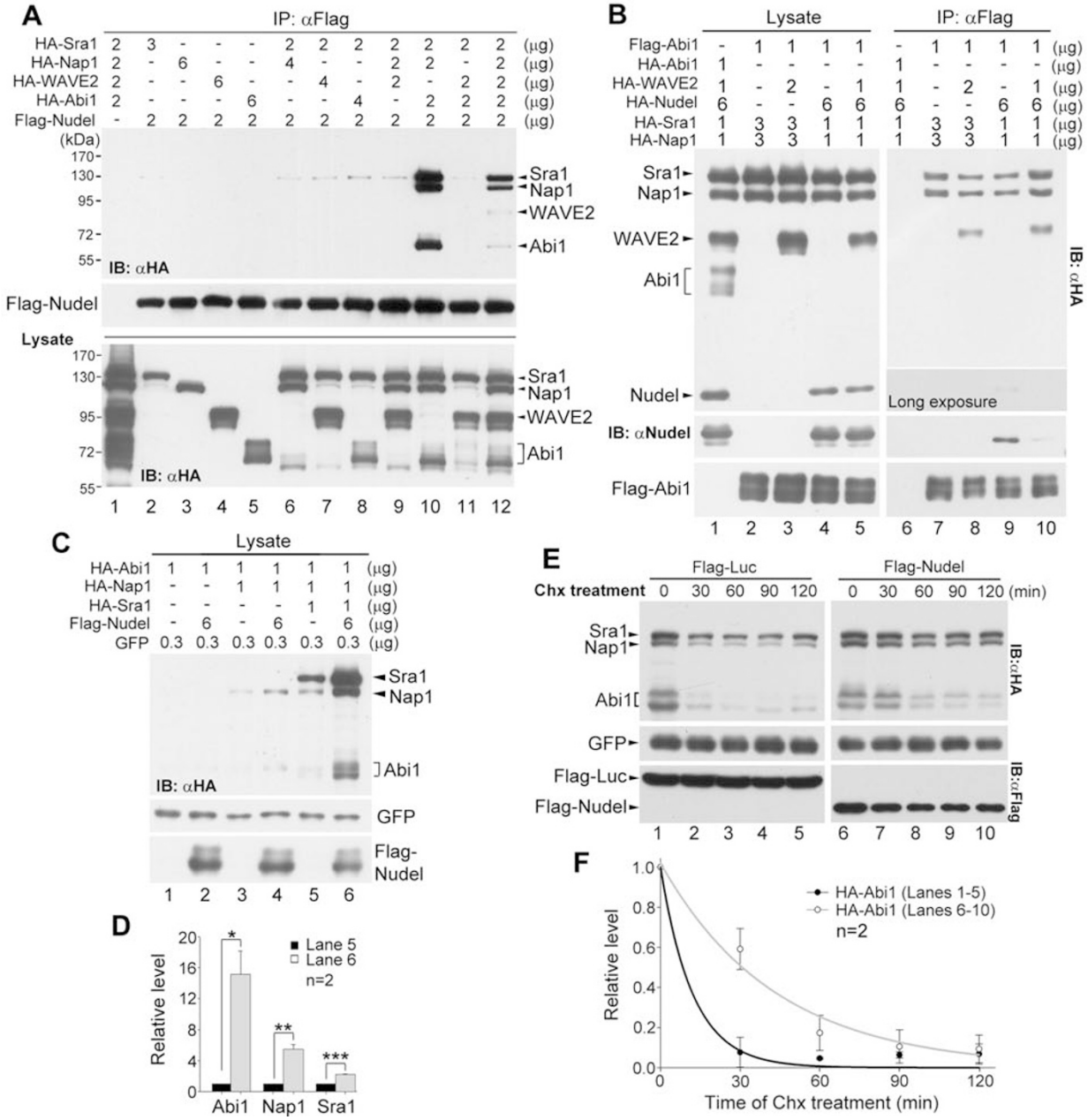

Figure 2 The impact of the Nudel-Sra1 interaction. **(A)** The effect of Nap1, Abi1, and WAVE2 on the Nudel-Sra1 interaction. HA-tagged WRC subunits were overexpressed to similar levels in the indicated combinations in HEK293T cells, together with Flag-Nudel. The amount of each expression plasmid used is listed. The cell lysates were subjected to co-IP with anti-Flag resin. **(B)** The effect of Nudel on associations of Sra1, Nap1, and WAVE2 with Abi1. HA-tagged proteins were overexpressed to similar levels as indicated, together with Flag-Abi1, in HEK293T cells. The cell lysates were subjected to co-IP with anti-Flag resin. **(C)** The levels of Sra1, Nap1, and Abi1 increased when Nudel was coexpressed. The indicated proteins were overexpressed with the indicated amount of each plasmid. GFP was used as a control for transfection efficiency. **(D)** The quantification results for the relative protein levels in lanes 5 and 6 of **C**. The protein levels were normalized to those of GFP. The values in lane 6 are then presented in arbitrary units relative to corresponding ones in lane 5. *, ** and *** represent $P \leq 0.05$, 0.01 and 0.001, respectively, in Student's *t*-tests. **(E)** Nudel increased the stability of the S-N-A complex. HEK293T cells were transfected as indicated in the lanes 5 and 6 of **C**, except that Flag-luciferase was expressed in the control cells. The cells were treated with 200 μg/ml of Chx at 36 h post transfection for the indicated times, followed by immunoblotting. **(F)** The quantification results for the relative protein levels of HA-Abi1 in **E**. The protein levels were normalized to those of GFP and presented relative to the values at 0 min.

the Nudel-HSPC300 interaction in the stabilization of HSPC300.

We then examined whether Nudel affected the turnover rate of HA-HSPC300. After the addition of Chx, we found that the levels of HA-HSPC300 decreased rapidly in control cells expressing Flag-luciferase (Figure 3C, lanes 1-5; Figure 3D). Its half-life was estimated to be 23 min on average (Figure 3D). In the presence of Flag-Nudel, however, HA-HSPC300 was quite stable, with a half-life of approximately 120 min (Figure 3C, lanes 6-10; Figure 3D).

As the substrates of the proteasome are often polyubiquitinated [26], we examined whether HA-HSPC300 was subjected to ubiquitination. Cells overexpressing HA-HSPC300 were then treated with MG132 for 12 h to enrich ubiquitinated proteins. When the cells were subjected to IP using the anti-HA resin, polyubiquitinated HA-HSPC300 was observed after immunoblotting using anti-ubiquitin antibody (Figure 3E, lane 2). Furthermore, the coexpression of Flag-Nudel markedly decreased the levels of polyubiquitinated HA-HSPC300 (Figure 3E, lanes 3 vs 2).

Nudel attenuates the subunit turnover of the HSPC300 oligomer through a tight interaction

The free pool of HSPC300 is reported to exist as homotrimers, implying that free monomer HSPC300 is unstable [3, 9]. Thus, it is possible that Nudel stabilizes HSPC300 (Figure 3) by repressing the dissociation of HSPC300 from its trimer. To test this idea, we examined whether Nudel-associated HSPC300 was devoid of the subunit turnover. When purified GST-HSPC300 was mixed with the HEK293T cell lysate containing HA-HSPC300, co-IP using the anti-HA resin showed that it potently formed hybrid oligomers with HA-HSPC300 (Figure 4A and 4B, lane 2), indicating an active subunit turnover between the oligomers. When GST-HSPC300 was mixed with the cell lysate containing both Flag-Nudel and HA-HSPC300, it mostly formed hybrid oligomers with the Nudel-free fraction of HA-HSPC300,

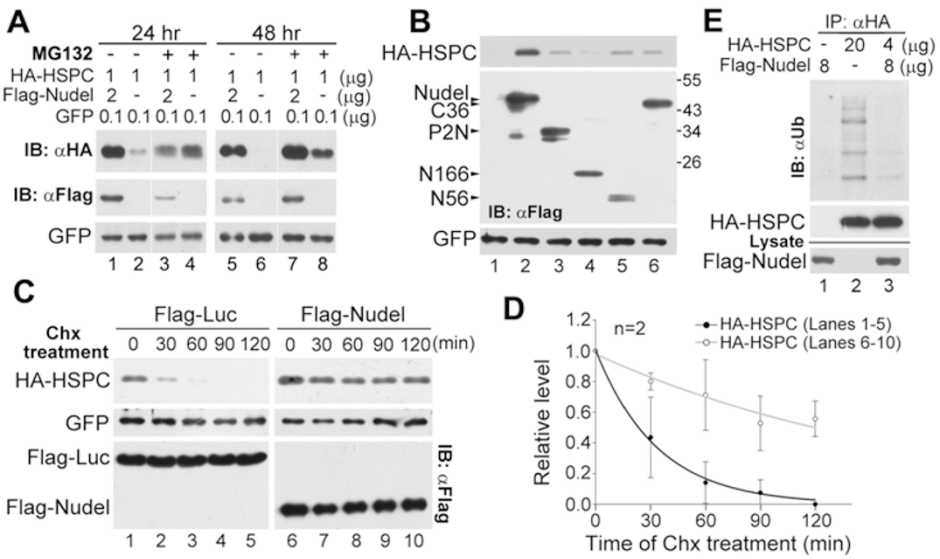

Figure 3 Nudel stabilizes HSPC300. **(A)** Nudel protected HSPC300 from the proteasome degradation. HEK293T cells were transfected with the indicated amount of plasmids to overexpress HA-HSPC300 and GFP with or without Flag-Nudel. The cells were harvested at the indicated time after 12 h of the MG132 treatment (5 μM), followed by immunoblotting (IB). GFP served as a control for the transfection efficiency. **(B)** Nudel mutants failed to stabilize HSPC300. HEK293T cells were transfected as indicated in **A** to transiently coexpress Flag-tagged Nudel or its mutants with HA-HSPC300. Cells were collected at 48 h post transfection for immunoblotting. A diagram for the Nudel mutants is shown in Supplementary information, Figure S2A. The effect of Nudel^{P2C}, which interacted with HSPC300 (Supplementary information, Figure S2A and S2C), was not examined due to its extremely low expression levels. **(C)** Nudel attenuated the turnover rate of HSPC300. HEK293T cells were transfected with the plasmids as indicated in **A**, except that Flag-luciferase was expressed in the control cells. The cells were treated with 200 μg/ml of Chx at 24 h post transfection for the indicated times, followed by immunoblotting. **(D)** The quantification results for the relative protein levels of HA-HSPC300 in **C**. Protein levels were normalized to that of GFP and presented relative to the values at 0 min. **(E)** Nudel attenuated the polyubiquitination of HSPC300. HEK293T cells transfected for 36 h to overexpress the indicated proteins were treated with MG132 for an additional 12 h. The cells were lysed in the RIPA buffer and then subjected to IP using the anti-HA resin.

whereas Flag-Nudel still predominantly associated with HA-HSPC300 (Figure 4A and 4B, lanes 4, 6), indicating that a tight interaction leads to a very low subunit turnover of the Nudel-associated HSPC300 oligomers.

When we mixed the cell lysate containing HA-HSPC300 with GST-HSPC300 and an increasing amount of Flag-Nudel, we found in the GST pull-down assays that Nudel inhibited the hybrid oligomer formation in a dose-dependent manner (Figure 4C). Furthermore, the potent interaction between Flag-Nudel and GST-HSPC300 (Figure 4C) excluded the possibility that the failure to detect GST-HSPC300 in lane 4 of Figure 4B was due to its incapability to bind to Flag-Nudel.

Nudel markedly promotes the HSPC300-WAVE2 interaction

As HSPC300 is able to directly bind to WAVE [10] and seems to complex with WAVE2 and Abi1 according to the WRC crystal structure [8], we examined whether Nudel could affect such interactions. We overexpressed Flag-HSPC300 with HA-tagged Nudel, WAVE2 and/or Abi1 in HEK293T cells as indicated (Figure 4D, lanes 2-8). Interestingly, in addition to Nudel, the overexpression of Abi1 and/or WAVE2 appeared to also stabilize HSPC300 (Figure 4D, lanes 2, 3, 5 vs 4), possibly due to the subcomplex formation [4, 5, 8, 10]. Co-IP using the anti-Flag M2 resin showed that the HSPC300-WAVE2 interaction was hardly detectable (Figure 4D, lane 11) even in the presence of HA-Abi1 (lane 13), unless Nudel was also ectopically coexpressed (Figure 4D, lanes 15, 16). Interestingly, although the level of HA-Abi1 exceeded that of HA-Nudel by approximately six-fold in the lysate (lane 8), HSPC300 and WAVE2 still preferentially associated with Nudel, instead of Abi1 (Figure 4D, lanes 8 vs 16).

Nudel is not present in the WRC

Our results indicated a strong association of Nudel with the S-N-A complex but not the S-N-A-W complex

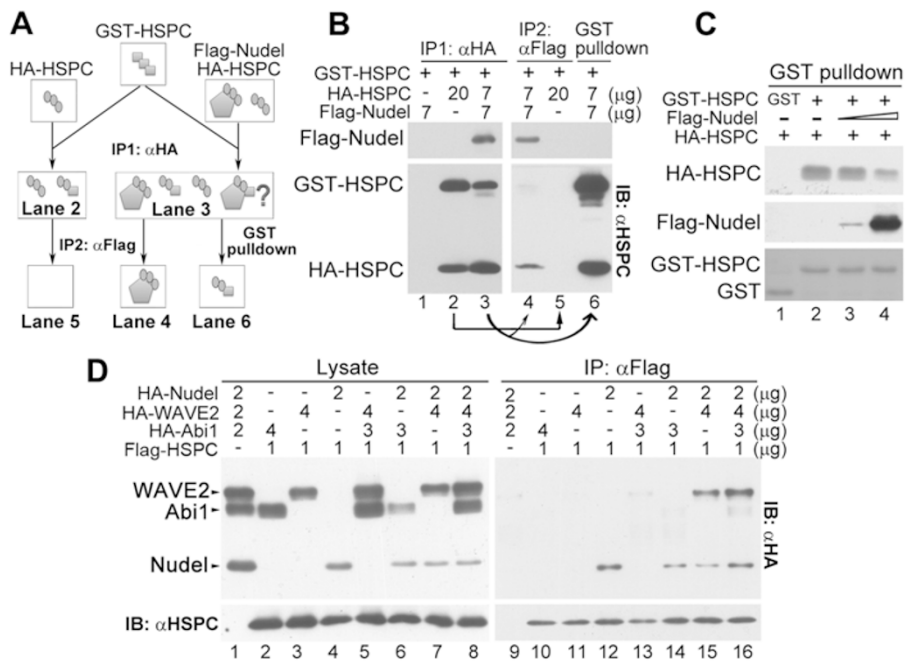

Figure 4 Nudel binds to HSPC300 tightly and facilitates the HSPC300-WAVE2 interaction. **(A)** A diagram summarizing the experiments and results in **B**. For simplicity, only representative complexes are displayed to assist understanding. **(B)** The Nudel-HSPC300 interaction was stable. HEK293T cells transfected as indicated to overexpress HA-HSPC300 and/or Flag-Nudel were lysed, mixed with GST-HSPC300 purified from *E. coli*, and subjected to the first round of co-IP (IP1) using the anti-HA resin (lanes 1-3). The immunoprecipitates eluted with the HA peptide were then subjected to the second round of co-IP (IP2) using the anti-Flag resin (lanes 4 and 5) or to the GST pull-down (lane 6) as indicated. **(C)** Nudel repressed the formation of the hybrid HSPC300 oligomer in a dose-dependent manner. HEK293T cell lysate containing HA-HSPC300 was mixed with purified GST, GST-HSPC, and Flag-Nudel as indicated, followed by the GST pull-down. Flag-Nudel was affinity-purified from HEK293T cell lysate using the anti-Flag resin and eluted with the Flag peptide. **(D)** Nudel promoted the WAVE2-HSPC300 interaction. HEK293T cells transfected with indicated amount of plasmids were lysed and subjected to co-IP with the anti-Flag resin.

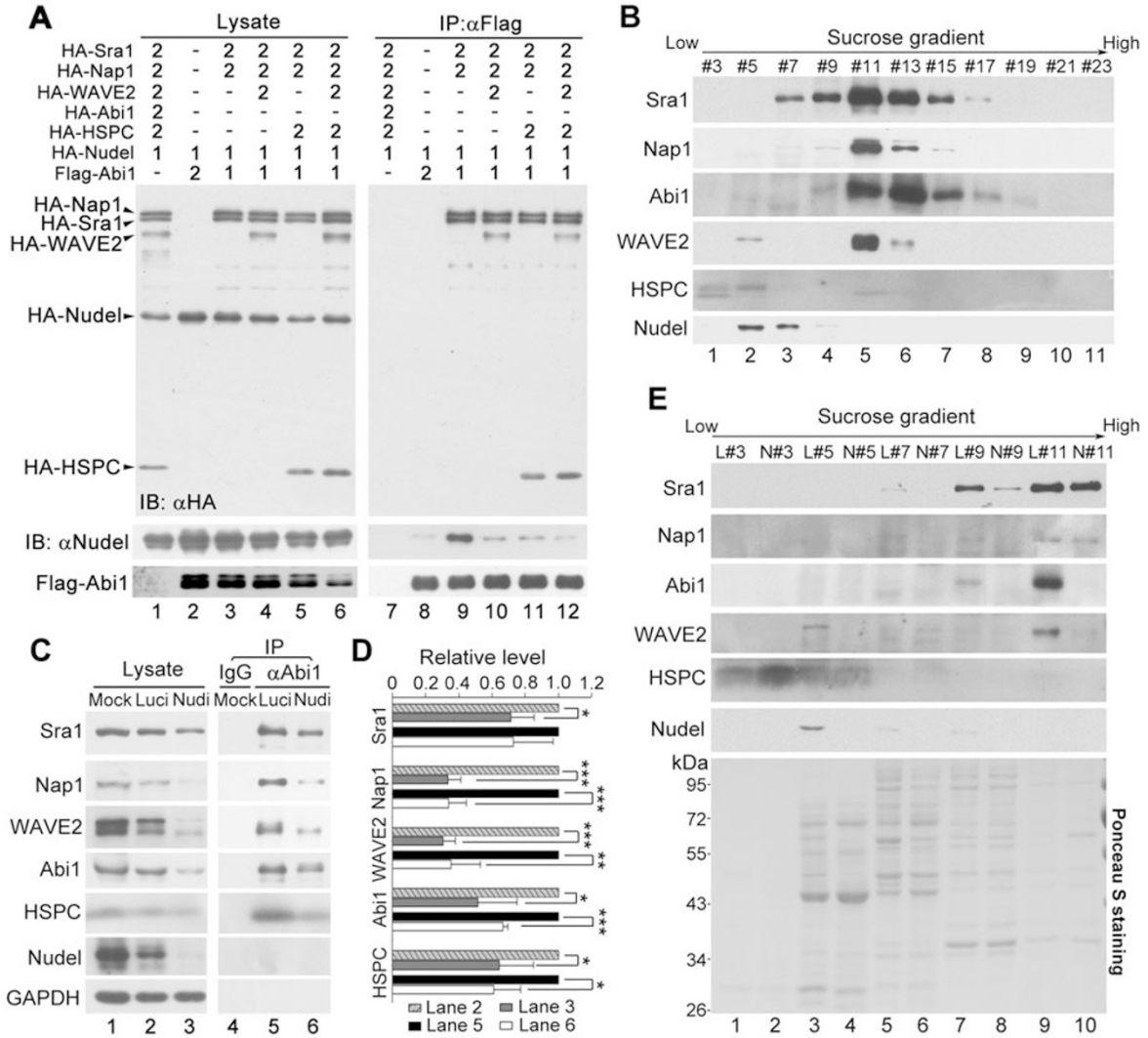

Figure 5 Depletion of Nudel downregulates the levels of the WRC. **(A)** Nudel was removed from the tetrameric subcomplexes as well as mature WRC. HEK293T cells transfected with the indicated amount of plasmids were lysed and subjected to co-IP with anti-Flag resin. **(B)** Endogenous Nudel and WRC did not coexist in the same fraction after sucrose gradient ultracentrifugation of HeLa cell lysate. **(C)** Nudel depletion attenuated the levels of both endogenous WRC subunits and mature WRC. HEK293T cells were transfected twice with the control (pTER-Luci) or Nudel RNAi (pTER-Nudi) plasmid, respectively, and harvested at 84 h. Lysates from equal number of cells (lanes 2 and 3) were subjected to co-IP with anti-Abi1 antibody (lanes 5 and 6), whereas lysate from untransfected cells (lane 1) was immunoprecipitated with normal IgG to serve as a control (lane 4). **(D)** The quantification results for the relative protein levels in **C**. The data were averaged from three independent experiments. *, **, and *** represent $P \leq 0.05$, 0.01, and 0.001, respectively, in Student's *t*-tests. **(E)** The levels of mature WRC were reduced in Nudel-depleted cells. HeLa cells were transfected twice with pTER-Luci or pTER-Nudi, respectively, and harvested at 84 h. After the sucrose gradient ultracentrifugation, the indicated fractions of control (L) and Nudel-depleted (N) lysates were subjected to SDS-PAGE. Equal loading of matched factions was confirmed by the Ponceacu S staining prior to immunoblotting.

(Figure 2A and 2B). To understand systematically how Nudel is involved in the later stages of the WRC assembly, Flag-Abi1 was overexpressed with HA-tagged proteins as shown in Figure 5A (lanes 2-6) and subjected to co-IP using the anti-Flag M2 resin. Immunoblotting indicated that similar to HA-WAVE2 (Figure 5A, lane 10; also see Figure 2B), HA-HSPC300 also formed a tetrameric complex with Sra1, Nap1, and Abi1 (Figure 5A, lane 11) [10]. When all five subunits were overexpressed, they formed the pentameric WRC (Figure

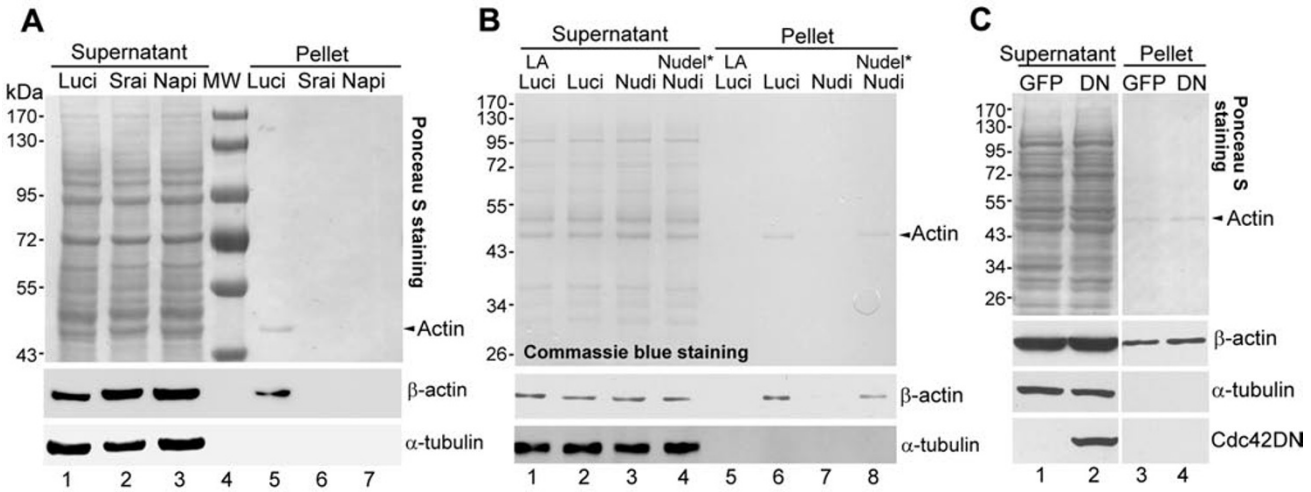

Figure 6 Depletion of Nudel abolishes the WRC-dependent *in vitro* actin polymerization. **(A)** The effect of the depletion of Sra1 or Nap1 by RNAi. HEK293T cells transfected with pTER-Luci or RNAi construct (pTER-Srai or pTER-Napi) were lysed at 72 h. After the induction of actin polymerization as described in Materials and Methods, the lysates were subjected to ultracentrifugation. Proteins in the supernatants and pellets were visualized by the Ponceau S staining and immunoblotting. **(B)** The effect of Nudel RNAi. HEK293T cells were transfected with the pTER-Luci, pTER-Nudi or pTER-Nudi plus an RNAi-resistant construct for Nudel expression (Nudel*) for 72 h. The cell lysates were subjected to the *in vitro* actin polymerization assays. Latruculin A (LA, 1 μg/ml) was used to inhibit nascent actin polymerization. **(C)** The effect of the dominant-negative Cdc42 mutant (DN). HEK293T cells overexpressing GFP or GFP-Cdc42DN were used for the *in vitro* actin polymerization assays. The composite lanes were cropped from the same gel or X-ray films.

5A, lane 12). Consistent with the results in Figure 2A and 2B, although Nudel strongly associated with the S-N-A complex (Figure 5A, lanes 9 vs 8), it was only weakly detected when the tetrameric or pentameric complex was formed (Figure 5A, lanes 10-12), indicating an unfavorable association of Nudel with these complexes.

To clarify whether Nudel associated with the mature WRC, we performed sucrose gradient ultracentrifugation with HeLa cell lysate. Similar to the previous report [10], the WRC in HeLa cells was mainly enriched in fraction #11 (Figure 5B), whereas free HSPC300 was seen in fractions #3-5 and a small portion of WAVE2 in fraction #5. By contrast, endogenous Nudel was abundant in factions #5-7 (lanes 2 and 3) but was not detected in faction #11 (lane 5), suggesting the absence of Nudel in mature WRC.

Depleting Nudel via RNAi attenuates the endogenous WRC

To verify a physiological role of Nudel in the WRC assembly *in vivo*, we silenced Nudel expression in HEK293T cells using a plasmid-based RNAi construct, pTER-Nudi [14, 15], and found a significant reduction in protein levels of the WRC (Figure 5C and 5D, lanes 3 vs 2). Notably, WAVE2 and Nap1 dropped to only about 30% of the wild-type levels (Figure 5C and 5D, lanes 3 vs 2). Co-IP from equal number of cells using anti-Abi1 antibody also revealed a similar reduction in the levels of Abi1 and its associated WRC subunits (Figure 5C and 5D, lanes 6 vs 5).

As anti-Abi1 antibody might also bring down subcomplexes in addition to mature WRC, we performed the sucrose gradient ultracentrifugation to better evaluate the levels of mature WRC in the Nudel-depleted cells. The absence of Nudel in fraction #5 indicated successful RNAi in HeLa cells (Figure 5E, lanes 4 vs 3). Abi1 and WAVE2 decreased to almost the basal levels in fraction #11 upon Nudel RNAi (Figure 5E, lanes 10 vs 9), indicating a lack of mature WRC. Sra1 and Nap1, however, were still similarly enriched in fraction #11 in both samples (Figure 5E, lanes 10 vs 9), possibly due to their associations with certain subcellular structures or other complex(es).

Nudel is required for the WRC-dependent actin polymerization

To investigate whether Nudel is involved in the WAVE-related actin polymerization, we developed a simple assay to induce the *in vitro* actin polymerizationin with HEK293T cell lysates (see Materials and Methods). The polymerized filamentous actin (F-actin) was then enriched by the ultracentrifugation. Such preparations were free of microtubule contaminants (Figure 6) and

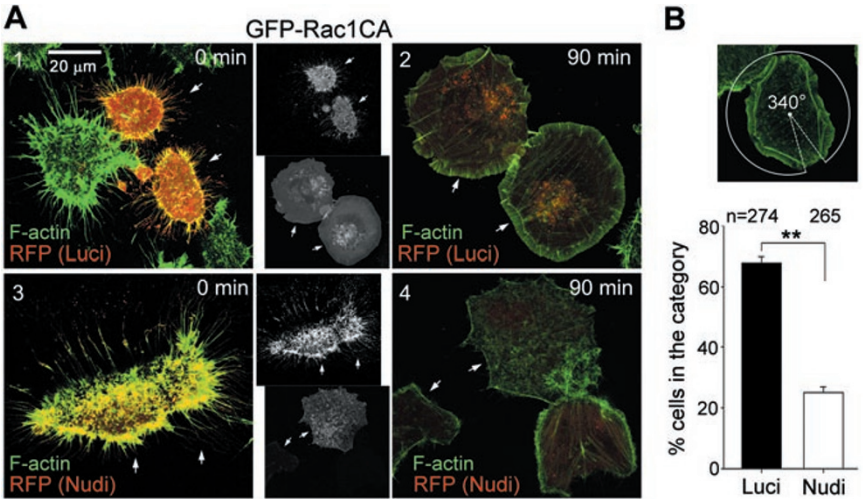

Figure 7 Depletion of Nudel impairs the formation of the lamellipodial F-actin. **(A)** Nudel-depleted cells lacked branched actin network at cell periphery during re-spreading. GFP-Rac1CA-positive ECV304 cells transfected with pTER-Luci-RFP or pTER-Nudi-RFP were treated with EDTA for 5 min and then allowed to re-spread prior to fixation at the indicated time. F-actin was visualized with Alexa Fluor 647-conjugated phalloidin. The arrows indicate the cells positive for both GFP and RFP. **(B)** The statistical results for cells with the lamellipodia coverage ≥ 270° at 90 min. The coverage was measured as the size of the circumference angle that covered the entire lamellipodia as demonstrated. $^{**}P \leq 0.01$ in Student's *t*-test.

β-actin was detected as the only protein band by the Ponceau S or Commassie blue staining (Figure 6A, lane 5; Figure 6B, lane 6). The β-actin band was eliminated in the presence of latruculin A (Figure 6B, lane 5), an actin polymerization inhibitor [27], confirming that the precipitated actin was indeed from F-actin, not from the monomer form of actin (G-actin) in the supernatant. More importantly, the F-actin formation was abolished after depletion of Sra1 or Nap1 by RNAi (Figure 6A, lanes 6 and 7 vs 5; Supplementary information, Figure S4A), indicating that the F-actin formation is a WRC-dependent process.

We thus knocked down Nudel by RNAi (Supplementary information, Figure S4B, lane 3) and found that the F-actin polymerization was also disrupted (Figure 6B, lanes 7 vs 6). Concomitant overexpression of GFP-Nudel using an RNAi-resistant construct (Supplementary information, Figure S4B, lane 4) [14] rescued the F-actin formation (Figure 6B, lanes 8 vs 7), thus excluding any off-target effect of the RNAi.

We have previously shown that Nudel RNAi results in the inactivation of Cdc42 [15]. To rule out possible influence of Cdc42, Cdc42DN, a dominant-negative mutant, was overexpressed in HEK293T cells (Figure 6C, lane 2) to inactivate the endogenous Cdc42 [28]. This, however, failed to affect F-actin polymerization (Figure 6C, lanes 4 vs 3). Therefore, the inhibitory effect of Nudel RNAi on the F-actin polymerization is attributed to the inactivation of the WRC.

Nudel knockdown impairs lamellipodial actin polymerization during cell spreading

We then investigated whether Nudel RNAi could inhibit the WRC-dependent actin polymerization in lamellipodia stimulated by Rac1CA, a constitutively active Rac1 [5, 14, 29]. As Nudel-depleted cells have weakened nascent adhesions and do not attach efficiently to the substratum [14], instead of using suspended cells for spreading assays [30], we treated attached ECV304 cells briefly with EDTA to induce partial cell shrinkage and then allowed them to re-spread [29]. After the EDTA treatment, cell bodies shrank, whereas numerous slender cytoplasmic projections rich in F-actin bundles, or retraction fibers [31], persisted in both the control and the Nudel RNAi cells (Figure 7A, panels 1 and 3). At 90 min after the removal of EDTA, an average of 67.7% of control cells showed a thick layer of branched actin network covering almost the entire cell periphery (≥ 270º of circumference angle) (Figure 7A, panel 2, arrows; Figure 7B) [14, 32]. By contrast, only 24.2% of the Nudel-knockdown cells showed the similarly well-developed lamellipodia (Figure 7B). The majority of Nudel-knockdown cells displayed mostly bundle-like F-actin, reminiscent of stress fibers, at the cell periphery (Figure 7A, panel 4, arrows); the branched actin network, if any, covered only ≤ 90º of circumference angle (Figure 7A,

panel 4) [14].

Discussion

We showed that Nudel is critical for the WRC assembly *in vivo*. Depletion of Nudel by RNAi resulted in the instability of the WRC subunits as well as the mature WRC (Figure 5C-5E), which phenocopied the depletion of any of the WRC subunits [3, 6, 9, 11-13]. Furthermore, the WRC-dependent actin polymerization *in vitro* was abolished and this phenotype was rescued by the reintroduction of Nudel (Figure 6). The WRC is activated by Rac [3, 5]. Consistently, the *in vitro* actin polymerization was not affected upon the inactivation of Cdc42 (Figure 6C), thus excluding the possibility that Nudel might impact actin polymerization through Cdc42 [15]. We have previously shown that Nudel RNAi abrogated lamellipodia formation in NIH3T3 and ECV304 cells, which can be rescued by the reintroduction of Nudel [14, 15]. Although the lack of Rac1CA-induced cell spreading after Nudel RNAi (Figure 7) could be partly attributed to the weakened nascent adhesions [14], the impaired lamellipodial actin polymerization in such cells (Figure 7) is in agreement with the lack of the mature WRC [6, 11, 13].

Our studies suggest a triple role of Nudel in the WRC assembly. First, Nudel potently protects the S-N-A complex against degradation via the physical interaction (Figures 2 and 8A). This effect, exerted through its direct binding to Sra1 (Figure 1 and Supplementary information, Figure S1), is robust and specific because when an equal amount of plasmid was used to express each subunit, a dramatic increase in the protein levels was only seen when the three subunits were simultaneously overexpressed with Nudel (Figure 2C and 2D). Furthermore, the much more dramatic interaction of Nudel with the S-N-A complex than with similar levels of Sra1 alone or its any other combinations with Nap1, Abi1, and/or WAVE2 (Figure 2A) suggests that the formation of the S-N-A complex might induce a conformational change in Sra1 to further favor its

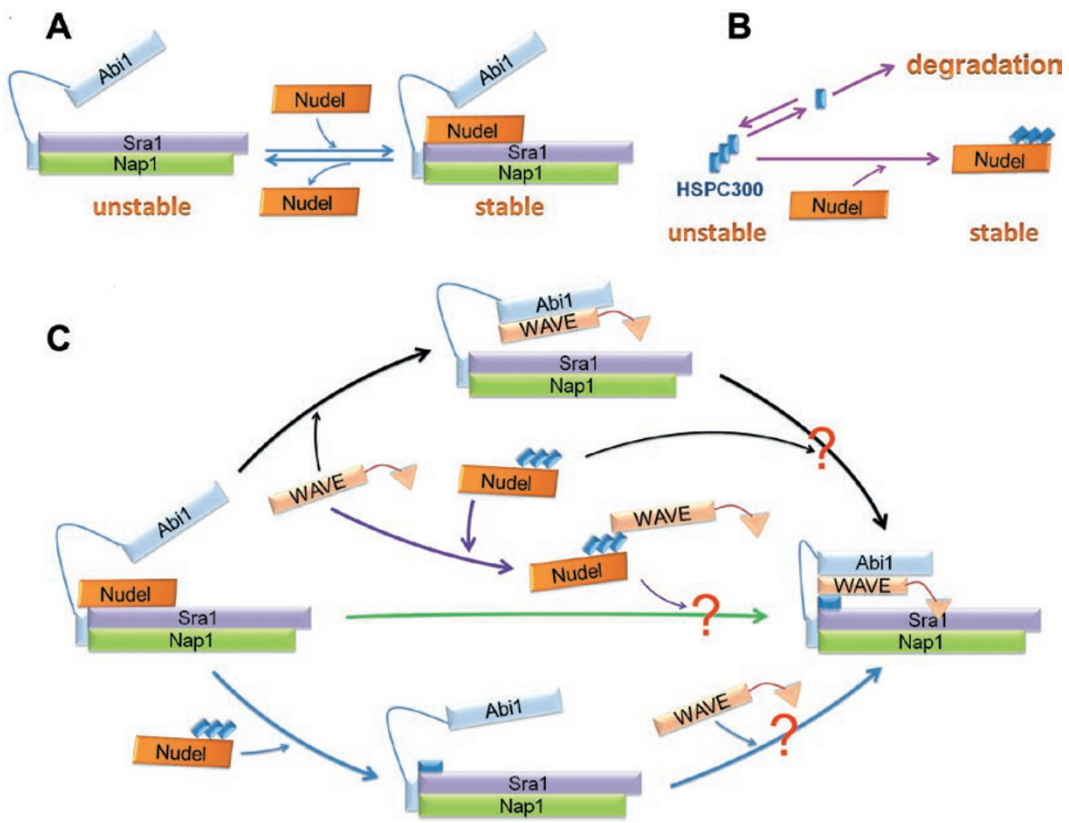

Figure 8 A model for the WRC assembly *in vivo*. **(A**, **B)** Nudel binds to and prevents the degradation of the S-N-A complex and HSPC300 homotrimer, respectively. The interaction of Nudel with HSPC300 is less dynamic than with the S-N-A complex. **(C)** The possible assembly paths of the WRC. All the intermediate complexes were verified in the study, though how they eventually form the mature WRC is speculative (the question marks). See the text for detailed discussions.

binding to Nudel. The S-N-A complex is not prone to dissociation, based on the nearly equal stoichiometry of Sra1, Nap1, and Abi1 in co-IP experiments (Figure 2A and 2B). Similarly, the subunits in the S-N-A-W and S-N-A-H complexes and the mature WRC are also very tightly associated (Figures 2B and 5A) [6, 10]. Such a feature makes the three subcomplexes ideal intermediates for the WRC assembly (Figure 8C). By contrast, the association of Nudel with the S-N-A complex is more dynamic than the interactions among the WRC subunits (Figure 2B, lane 9 and Figure 8A). Its associations with the two tetrameric subcomplexes, if any, were even weaker (Figure 2A, lanes 12 vs 10; Figure 2B, lanes 10 vs 9; Figure 5A, lanes 10 and 11 vs 9). The fractionation results further suggest that Nudel is not present in the mature WRC (Figure 5B, lane 5). Nudel is therefore probably involved in the early steps of the WRC assembly, but not in the WRC function (Figure 8).

Second, Nudel interacts tightly with HSPC300 and protects HSPC300 against polyubiquitination and the proteasome-mediated degradation (Figures 1, 3, 4 and 8B). Such an effect appears prominent because the half-life of HA-HSPC300 increased by an average of 5.2-fold in the presence of Flag-Nudel (Figure 3C and 3D). Moreover, the stabilization effect requires the direct interaction of HSPC300 with Nudel (Figure 3B). Since the free pool of HSPC300 exists as homotrimers and the monomeric HSPC300 may be unstable in cells [3, 9], we postulate that Nudel exerted the stabilization effect on HSPC300 by binding to the trimeric form (Figures 4A and 8). In this context, the lack of the hybrid oligomer formation in the Nudel-associated pool of HSPC300 (Figure 4A-4C) can be attributed to the tight Nudel binding-mediated repression of the otherwise active dissociation of HSPC300 from its oligomer (Figure 8B). Such a dramatic reduction in the subunit turnover rate thus prevented the degradation of HSPC300 in the form of unstable monomer (Figure 8B) [9]. Nevertheless, if Nudel actually binds to the monomeric HSPC300, it may directly stabilize such a form.

The third role of Nudel lies in its ability to dramatically enhance the H-W interaction (Figures 4D and 8C), possibly through an allosteric effect on HSPC300. In the ultracentrifugation experiments, endogenous Nudel also distributed with endogenous WAVE2 and HSPC300 in faction #5 (Figure 5B and 5E), supporting the existence of such an intermediate in HeLa cells. Interestingly, although the W-H-A complex has been used to successfully assemble the mature WRC *in vitro* [4, 8], this complex was only barely seen in our co-IP experiments as compared to the much more abundant Nudel-H-W complex (Figure 4D), possibly due to its inefficient assembly or rapid degradation in cells. In contrast, the Nudel-H-W complex was much more stable. Since the recruitment of WAVE2 did not affect the Nudel-HSPC300 interaction in co-IP (Figure 4D), it is likely that HSPC300 still remained as a trimer in the Nudel-H-W complex (Figure 8C), though there may be other possibilities.

We thus propose three *in vivo* assembly paths of the WRC that use different intermediates (Figure 8C). The middle path involves only two intermediate complexes whose assembly and/or stability was highly stimulated by Nudel (Figures 2-4), and might thus be the most efficient. The bottom path, however, could be superior in preventing uncontrolled activities of free WAVE protein and other WAVE-containing intermediates (Figure 8C) [4, 5, 8, 10]. This pathway may appear dominant if free WAVE becomes a limiting factor. The importance of Nudel in the early stages of the WRC assembly also explains why Nudel is not required for the *in vitro* WRC assembly [4, 8]. The biochemical details of the proposed model need to be further investigated in the future.

Why the Nudel binding can stabilize the S-N-A complex and HSPC300 is currently not clear. Possible insights include functions as a chaperone to facilitate the correct folding of Sra1 and HSPC300 or as a shield to hinder the attack by the protein degradation machineries. As implicated in our overexpression experiments, Nudel may be especially critical for cells that require abundant WRC. In addition to the suggested roles of Nudel in the WRC assembly (Figure 8), we cannot exclude the possibility that the Nudel-associated Sra1, HSPC300, and their related subcomplexes may have other functions. For instance, as Nudel has been shown to serve as a cargo protein-docking site in the dynein motor [21], it might affect the spatiotemporal distributions of its associated subcomplexes via the dynein-mediated retrograde transport to prevent their deleterious activities [4, 8] at the cell periphery.

How the different Nudel functions are coordinated is also not known. Nudel is a multifunctional protein. Domain mapping experiments suggest that, although Nudel interacts with Lis1 through its N-terminal domain, many of the Nudel-associated proteins, including dynein, Cdc42GAP, paxillin, Sra1, and HSPC300, bind to the overlapping C-terminal regions of Nudel because they all require the same region deleted in the C36 mutant for the interaction (Supplementary information, Figure S2) [14, 15, 19, 33]. Our previous results suggest synergistic interactions of Cdc42GAP and paxillin with Nudel, which may couple the high Cdc42 activity and the tight nascent adhesions to the same spatial locations at the leading edge for an orchestrated cell migration

[14]. Therefore, different partners may bind to Nudel separately, competitively, or synergistically to ensure proper functions.

Materials and Methods

Plasmid constructs

The expression plasmids for Flag-tagged firefly luciferase and human Nudel and mutants, GFP-tagged Nudel for rescue experiment, Rac1Q61L (Rac1CA), and Cdc42T17N (Cdc42DN) were described previously [14, 19, 34, 35]. The expression plasmids for HA-tagged WAVE2, Nap1, Abi1, and HSPC300 were gifts from Dr Alexis Gautreau (Institut Curie, France) [10]. The expression plasmid for Myc-Sra1 was kindly provided by Dr Jean-Louis Mandel (Universite Louis Pasteur, France) [36]. Others were constructed by inserting PCR-amplified ORFs into pCS2+-HA, pCDNA3-Flag, pET28a or pGEX-2T.

pTER-Nudi, pTER-Luci, pTER-Nudi-RFP, and pTER-Luci-RFP, the latter two of which also express RFP as a transfection marker, were also used to express shRNA against Nudel or firefly luciferase [14, 37]. Other RNAi constructs were generated using pTER$^+$ vector [38] and published targeting sequences (5'-GTACTCCAACAAGGACTGC-3' for human Sra1; 5'–CCAGATTGCTGCAGCTTTG-3' for human Nap1) [13]. All the newly constructed plasmids were confirmed by sequencing.

Antibodies and reagents

Commercial antibodies used were monoclonal antibody against α-tubulin, β-actin, Flag-tag, HA-tag, His-tag (Sigma, Saint Louis, USA), Cdc42 (Santa Cruz Biotechnology, USA), and GST (Wolwo Biotech Co., Shanghai, China); rabbit antibodies against GFP, human WAVE2 (Santa Cruz Biotechnology), Abi1 (Sigma), and Nap1 (Ptg Lab, China). Affinity-purified anti-Nudel IgY was prepared as described [37]. Rabbit antibodies against human Sra1 or HSPC300 were raised using bacterially expressed His-Sra1 (1-401 aa) or His-HSPC300, and then affinity-purified using GST-tagged proteins. Anti-Flag M2 resin and anti-HA resin were obtained from Sigma. Alexa Fluor 647-conjugated phalloidin and goat secondary antibodies conjugated with horseradish peroxidase were from Invitrogen (Carlsbad, CA, USA). Latrunculin A, nocodazole, cycloheximide (CHX) and MG132 were from Sigma.

Cell culture and transfection

Cells were cultured in Dulbecco's modified Eagle's medium (Invitrogen) supplemented with 10% (v/v) bovine serum (Sijiqing, Hangzhou, China) at 37 ºC in an atmosphere containing 5% CO_2. For protein overexpression, cells were transfected using the conventional calcium phosphate method and harvested at ~48 h post transfection. For RNAi, HEK293T and HeLa cells were transfected using Lipofectamine 2000 (Invitrogen) and either harvested at 72 h or subjected to the second round of transfection at ~48 h by using the calcium phosphate method and collected at ~84 h. For the re-spreading experiments, ECV304 cells were transfected with RNAi constructs using Lipofectamine 2000 for 48 h, followed by the second round of transfection to express GFP-Rac1CA for another 24 h. Cells were then treated with 0.02% EDTA in PBS for 5 min, rinsed with PBS, and cultured in the medium supplemented with 10% (v/v) fetal bovine serum (Sijiqing) to stimulate re-spreading [29].

Immunoprecipitation, GST pull-down, and immunoblotting

Co-IP and GST pull-down were performed as described previously [14, 15]. When the anti-Flag or anti-HA beads were used for IP, associated proteins were eluted with the Flag or HA peptide, respectively. For IB, proteins were resolved by SDS-PAGE and transferred to nitrocellulose membranes (Schleicher & Schuell, Keene, USA). Immunoblots were developed in chemiluminescence reagent (Perkin Elmer, Boston, USA) and exposed to X-ray films (Kodak, New York, USA). Relative protein level was quantified by subtracting the background intensity from the total intensity within a rectangle that just covered the protein band of interest in an immunoblot using Adobe Photoshop and then normalized the value to that of the corresponding loading control. Results were presented as mean ± SD. The curve fitting and protein half-life estimation were performed as described [39].

In vitro actin polymerization

2×10^7 HEK293T cells were trypsinized and re-suspended in one volume of HEPES buffer (50 mM HEPES, pH 7.5, 50 mM NaCl, 1 mM $MgCl_2$, 2 mM EGTA, 1 mM DTT, 10 μg/ml nocodazole, and protease inhibitors). The cells were lysed by passing through a 1-ml syringe with a 26 G needle for 60 times, and spun at 13 200 rpm for 30 min in a 4 ºC bench top centrifuge [40]. The supernatant was further clarified at 221 000× *g* for 60 min at 4 ºC to remove pre-existing F-actin [41]. After the addition of GTP (1 mM), ATP (1 mM), and creatine phosphate (7.5 mM), the mixture was incubated for 60 min at 37 ºC to induce actin polymerization [42]. Finally the mixture was layered onto pre-warmed 10% (m/v) sucrose cushion in the HEPES buffer, and centrifugated at 40 000× *g* for 30 min at 37 ºC to sediment F-actin [40, 43]. The pellets were rinsed twice with the buffer and dissolved in SDS loading buffer.

Sucrose gradient ultracentrifugation

Sucrose gradient ultracentrifugation was performed as described previously [10] with minor modifications. Briefly, 1×10^7 HeLa cells were lysed by nitrogen cavitation. In all, 400 μl of the clarified supernatant was laid on the top of the sucrose gradient prepared by the freeze-thaw method (15% sucrose solution frozen at -70 ºC overnight and thawed at 4 ºC) [44]. The gradients were run for 17 h at 40 000 rpm with a SW40 rotor (Beckman Coulter). Fractions of 0.5 ml each were collected from the top of the gradient.

Microscopy

Cells grown on sterile glass coverslips were fixed with 4% paraformaldehyde (Sigma-Aldrich) for 15 min, followed by the permeabilization with 0.5% Triton X-100 (v/v) for 10 min. Fluorescence images were captured using a Leica TCS SP5 laser-scanning confocal microscope.

Lamellipodia coverage was measured with ImageJ (NIH). Statistical data were from at least two independent experiments and presented as mean ± SD.

Acknowledgments

We thank Yan Li, Lihou Yu, Qiangge Zhang, Fubin Wang,

Qiongping Huang, Jing Guo, Zhenye Yang, Jun Chen, Shengjie Xue, and Jianqun Zheng for technical assistance. We also thank Dr Xiumin Yan and Yidong Shen for advice on experiment design and critical reading of the manuscript, Dr Alexis Gautreau (Institut Curie, France) for expression plasmids of the WRC subunits, and Dr Xiaobing Yuan (Institute of Neuroscience, SIBS, CAS) for small GTPase constructs. This work was supported by the National Basic Research Program of China (2010CB912102 and 2012CB945003), the National Natural Science Foundation of China (30830060 and 31010103910), Chinese Academy of Sciences (XDA01010107), and Science and Technology Commission of Shanghai Municipality (09JC1416200).

References

1 Goley ED , Welch MD. The ARP2/3 complex: an actin nucleator comes of age. *Nat Rev Mol Cell Biol* 2006; **7**:713-726.
2 Takenawa T, Suetsugu S. The WASP-WAVE protein network: connecting the membrane to the cytoskeleton. *Nat Rev Mol Cell Biol* 2007; **8**:37-48.
3 Derivery E., Gautreau A. Generation of branched actin networks: assembly and regulation of the N-WASP and WAVE molecular machines. *Bioessays* 2010; **32**:119-131.
4 Ismail AM, Padrick SB, Chen B, Umetani J, Rosen MK. The WAVE regulatory complex is inhibited. *Nat Struct Mol Biol* 2009; **16**:561-563.
5 Eden S, Rohatgi R, Podtelejnikov AV, Mann M, Kirschner MW. Mechanism of regulation of WAVE1-induced actin nucleation by Rac1 and Nck. *Nature* 2002; **418**:790-793.
6 Innocenti M, Zucconi A, Disanza A, *et al.* Abi1 is essential for the formation and activation of a WAVE2 signalling complex. *Nat Cell Biol* 2004; **6**:319-327.
7 Derivery E, Lombard B, Loew D, Gautreau A. The Wave complex is intrinsically inactive. *Cell Motil Cytoskel* 2009; **66**:777-790.
8 Chen Z, Borek D, Padrick SB, *et al.* Structure and control of the actin regulatory WAVE complex. *Nature* 2010; **468**:533-538.
9 Derivery E, Fink J, Martin D, *et al.* Free Brick1 is a trimeric precursor in the assembly of a functional wave complex. *PLoS One* 2008; **3**:e2462.
10 Gautreau A, Ho HY, Li J, Steen H, Gygi SP, Kirschner MW. Purification and architecture of the ubiquitous Wave complex. *Proc Natl Acad Sci USA* 2004; **101**:4379-4383.
11 Kunda P, Craig G, Dominguez V, Baum B. Abi, Sra1, and Kette control the stability and localization of SCAR/WAVE to regulate the formation of actin-based protrusions. *Curr Biol* 2003; **13**:1867-1875.
12 Rogers SL, Wiedemann U, Stuurman N, Vale RD. Molecular requirements for actin-based lamella formation in Drosophila S2 cells. *J Cell Biol* 2003; **162**:1079-1088.
13 Steffen A, Rottner K, Ehinger J, *et al.* Sra-1 and Nap1 link Rac to actin assembly driving lamellipodia formation. *EMBO J* 2004; **23**:749-759.
14 Shan Y, Yu L, Li Y, *et al.* Nudel and FAK as antagonizing strength modulators of nascent adhesions through paxillin. *PLoS Biol* 2009; **7**:e1000116.
15 Shen Y, Li N, Wu S, *et al*. Nudel binds Cdc42GAP to modulate Cdc42 activity at the leading edge of migrating cells. *Dev Cell* 2008; **14**:342-353.
16 Etienne-Manneville S. Cdc42--the centre of polarity. *J Cell Sci* 2004; **117**:1291-1300.
17 Kardon JR, Vale RD. Regulators of the cytoplasmic dynein motor. *Nat Rev Mol Cell Biol* 2009; **10**:854-865.
18 Shu TZ, Ayala R, Nguyen MD, Xie Z, Gleeson JG, Tsai LH. Ndel1 operates in a common pathway with LIS1 and cytoplasmic dynein to regulate cortical neuronal positioning. *Neuron* 2004; **44**:263-277.
19 Liang Y, Yu W, Li Y, *et al*. Nudel functions in membrane traffic mainly through association with Lis1 and cytoplasmic dynein. *J Cell Biol* 2004; **164**:557-566.
20 Shu T, Ayala R, Nguyen MD, Xie Z, Gleeson JG, Tsai LH. Ndel1 operates in a common pathway with LIS1 and cytoplasmic dynein to regulate cortical neuronal positioning. *Neuron* 2004; **44**:263-277.
21 Nguyen MD, Shu T, Sanada K, *et al.* A NUDEL-dependent mechanism of neurofilament assembly regulates the integrity of CNS neurons. *Nat Cell Biol* 2004; **6**:595-608.
22 Liang Y, Yu W, Li Y, *et al*. Nudel modulates kinetochore association and function of cytoplasmic dynein in M phase. *Mol Biol Cell* 2007; **18**:2656-2666.
23 Zhang Q, Wang F, Cao J, *et al*. Nudel promotes axonal lysosome clearance and endo-lysosome formation via dynein-mediated transport. *Traffic* 2009; **10**:1337-1349.
24 Li Y, Yu W, Liang Y, Zhu X. Kinetochore dynein generates a poleward pulling force to facilitate congression and full chromosome alignment. *Cell Res* 2007; **17**:701-712.
25 Janas JA, Van Aelst L. Oncogenic tyrosine kinases target Dok-1 for ubiquitin-mediated proteasomal degradation to promote cell transformation. *Mol Cell Biol* 2011; **31**:2552-2565.
26 Sorokin AV, Kim ER, Ovchinnikov LP. Proteasome system of protein degradation and processing. *Biochemistry* 2009; **74**:1411-1442.
27 Spector I, Shochet NR, Kashman Y, Groweiss A. Latrunculins: novel marine toxins that disrupt microfilament organization in cultured cells. *Science* 1983; **219**:493-495.
28 Kozma R, Sarner S, Ahmed S, Lim L. Rho family GTPases and neuronal growth cone remodelling: relationship between increased complexity induced by Cdc42Hs, Rac1, and acetylcholine and collapse induced by RhoA and lysophosphatidic acid. *Mol Cell Biol* 1997; **17**:1201-1211.
29 Price LS, Leng J, Schwartz MA, Bokoch GM. Activation of Rac and Cdc42 by integrins mediates cell spreading. *Mol Biol Cell* 1998; **9**:1863-1871.
30 Cuvelier D, Théry M, Chu YS, *et al.* The universal dynamics of cell spreading. *Curr Biol* 2007; **17**:694-699.
31 Thery M, Bornens M. Cell shape and cell division. *Curr Opin Cell Biol* 2006; **18**:648-657.
32 Hall A. Rho GTPases and the actin cytoskeleton. *Science* 1998; **279**:509-514.
33 Sasaki S, Shionoya A, Ishida M, *et al*. A LIS1/NUDEL/cytoplasmic dynein heavy chain complex in the developing and adult nervous system. *Neuron* 2000; **28**:681-696.
34 Ding C, Liang X, Ma L, Yuan X, Zhu X. Opposing effects of Ndel1 and alpha1 or alpha2 on cytoplasmic dynein through competitive binding to Lis1. *J Cell Sci* 2009; **122**:2820-2827.
35 Yan X, Li F, Liang Y, *et al*. Human Nudel and NudE as

regulators of cytoplasmic dynein in poleward protein transport along the mitotic spindle. *Mol Cell Biol* 2003; **23**:1239-1250.
36 Schenck A, Bardoni B, Moro A, Bagni C, Mandel JL. A highly conserved protein family interacting with the fragile X mental retardation protein (FMRP) and displaying selective interactions with FMRP-related proteins FXR1P and FXR2P. *Proc Natl Acad Sci USA* 2001; **98**:8844-8849.
37 Guo J, Yang Z, Song W, *et al*. Nudel contributes to microtubule anchoring at the mother centriole and is involved in both dynein-dependent and -independent centrosomal protein assembly. *Mol Biol Cell* 2006; **17**:680-689.
38 van de Wetering M, Oving I, Muncan V, *et al*. Specific inhibition of gene expression using a stably integrated, inducible small-interfering-RNA vector. *EMBO Rep* 2003; **4**:609-615.
39 Eden E, Geva-Zatorsky N, Issaeva I, *et al.* Proteome half-life dynamics in living human cells. *Science* 2011; **331**:764-768.
40 Paschal BM, Shpetner HS Vallee RB. MAP 1C is a microtubule-activated ATPase which translocates microtubules *in vitro* and has dynein-like properties. *J Cell Biol* 1987; **105**:1273-1282.
41 Kikuchi M, Maruyama K, Noda H. Sedimentation behavior of F-actin of various types. *J Biochem* 1974; **75**:1103-1111.
42 Ma L, Cantley LC, Janmey PA, Kirschner MW. Corequirement of specific phosphoinositides and small GTP-binding protein Cdc42 in inducing actin assembly in *Xenopus* egg extracts. *J Cell Biol* 1998; **140**:1125-1136.
43 Correas I, Padilla R, Avila J. The tubulin-binding sequence of brain microtubule-associated proteins, tau and MAP-2, is also involved in actin binding. *Biochem J* 1990; **269**:61-64.
44 Centelles JJ, Franco R. Heterogeneity of the gradients performed by the freeze-thaw method. *J Biochem Biophys Methods* 1989; **18**:177-182.

(**Supplementary information** is linked to the online version of the paper on the *Cell Research* website)